CHEMMEDCHEM

DOI: 10.1002/cmdc.200700269

Peptide-Containing Aggregates as Selective Nanocarriers for Therapeutics

Antonella Accardo,[b] Diego Tesauro,[b] Luigi Aloj,[c] Laura Tarallo,[c] Claudio Arra,[d] Gaetano Mangiapia,[a] Mauro Vaccaro,[a] Carlo Pedone,[b] Luigi Paduano,*[a] and Giancarlo Morelli*[b]

New nanocarriers are obtained by assembling two amphiphilic monomers: one containing the bioactive peptide CCK8 spaced, by a polydisperse poly(ethylene glycol), from two hydrophobic tails ((C18)2PEG2000CCK8), and the other containing a chelating agent able to give stable radiolabeled indium-111 complexes linked to the same hydrophobic moiety ((C18)2DTPAGlu). The size and shape of the supramolecular aggregates were structurally characterized by dynamic light scattering, small-angle neutron scattering, and cryogenic transmission electronic microscopy. Under the experimental conditions we investigated (pH 7.4 and molar ratio between monomers 30:70), there is the presence of high polydisperse aggregates: rod-like micelles with a radius of ~40 Å and length >700 Å, open bilayer fragments with thickness ~65 Å, and probably vesicles. The presence of the bioactive peptide well exposed on the external surface of the aggregate allows selective targeting of nanocarriers towards the cholecystokinin receptors overexpressed by the cancerous cells. In vitro binding assays and in vivo biodistribution studies by nuclear medicine experiments using indium-111 are reported. Moreover, preliminary data concerning the drug loading capability of the aggregates and their drug efficiency on the target cells is reported by using the cytotoxic drug doxorubicin. Incubation of receptor-positive and control cells with peptide-containing aggregates filled with doxorubicin shows significantly lower cell survival in receptor-expressing cells relative to the control, for samples incubated in the presence of doxorubicin.

Introduction

Systemic administration of pharmaceuticals is frequently used in modern medicine.[1] In the last decade, supramolecular aggregates such as micelles and vesicles have attracted great attention for their potential application as carriers in drug delivery. Their base requirements in systemic administration include high drug-loading capacity, biodegradability, prolonged circulation times, slow plasma clearance, and controllable drug-release profiles.[2,3] The hydrophobic core of micelles and the inner cavity of vesicles are carrier compartments that can accommodate large amounts of drug, whereas the shell, consisting of a brush-like protecting corona, stabilizes them in aqueous solutions. To increase therapeutic or diagnostic efficacy of the administered drug and reduce potential toxic side effects on non-target organs, the development of schemes aimed at achieving more specific and selective delivery to target cells constitutes a major challenge for many clinical applications. In particular, applications of such schemes would be of great interest for the management of patients affected by cancer.

The targeting capabilities of peptides and antibodies raised against a specific molecular target have been proposed to achieve such selective delivery.[4,5] Antibodies show very high selectivity for their antigens but present some drawbacks such as a slow extravasation process due to their high molecular weight.[6] Moreover, high-molecular-weight molecules, such as immunoglobulins (150 kDa), have very slow capillary permeability which prevent them from reaching the target molecules with ideal timing.

The use of peptides as targeting tools has been validated in a number of applications.[7,8] One example are radiolabeled peptides which are used in nuclear medicine techniques to perform imaging or to deliver radiotherapeutic doses to cancer tissues, overexpressing particular types of receptors such as those for somatostatin.[9] In this case, a simple entity such as the radionuclide is driven by the peptide to target cells at higher concentrations compared to non-target organs. A more

[a] *Dr. G. Mangiapia, Dr. M. Vaccaro, Prof. L. Paduano*
Department of Chemistry, University of Naples "Federico II"
Via Cynthia, 80126 Napoli (Italy)
Fax: (+39) 081-674-090

[b] *Dr. A. Accardo, Dr. D. Tesauro, Prof. C. Pedone, Prof. G. Morelli*
CIRPeB, Department of Biological Sciences & IBB CNR
University of Naples "Federico II"
Via Mezzocannone 16, 80134 Napoli (Italy)
Fax: (+39) 081-253-6642
E-mail: gmorelli@unina.it

[c] *Dr. L. Aloj, Dr. L. Tarallo*
Department of Nuclear Medicine
Istituto Nazionale per lo Studio e la Cura dei Tumouri
Fondazione "G. Pascale"
Via M. Semmola, 80131 Napoli (Italy)

[d] *Dr. C. Arra*
Department of Animal Experimentation
Istituto Nazionale per lo Studio e la Cura dei Tumouri
Fondazione "G. Pascale"
Via M. Semmola, 80131 Napoli (Italy)

Supporting information for this article is available on the WWW under http://www.chemmedchem.org or from the author.

complex and challenging objective would be to adopt a similar scheme to deliver supramolecular aggregates, such as micelles or vesicles, to a tissue of interest. Such aggregates, as mentioned above, could be used as nanovectors for large quantities of drugs contained in the inner cavity of the supramolecular aggregate. Examples of target specific supramolecular aggregates, employed as vectors of drugs or metal complexes, include micelles and vesicles loaded with poorly soluble anticancer agents[4,10] or bearing Gd^{III} complexes.[11,12] In these cases the aggregates are externally modified with tumor specific antibodies.

An effective way to prepare supramolecular aggregates modified on the surface with a reporter compound is the mixed assembling of different monomers. With this strategy, we have recently developed mixed aggregate systems, acting as high relaxivity MRI contrast agents,[13–15] formed by two different amphiphilic monomers, one containing a bioactive peptide and the other a chelating moiety capable of forming stable complexes with Gd(III) ions.

We have now developed new mixed aggregates with enhanced properties and studied them as potential target selective nanovectors of drugs. The new nanovectors are obtained by mixing the monomers reported in Figure 1. The lipophilic moiety of both monomers, consisting of two C_{18} alkyl chains, allows the formation of the aggregates, whereas the CCK8 peptide and the anionic DTPAGlu chelating agent remain mainly exposed on the nanovector external surface. CCK8 is the C-terminal sequence of the cholecystokinin hormone and provides the binding sequence for the cholecystokinin receptor subtypes 1 and 2 (CCK_1-R and CCK_2-R): its binding affinity toward the two receptors is in the nanomolar range.[16] Overexpression of both of these receptor subtypes has been demonstrated in certain human tumors.[17] To obtain adequate distancing of the bioactive peptide from the surface of the supramolecular aggregate, and reduce potential hindrance to its specific binding activity, a hydrophilic spacer is introduced between the N terminus of the peptide and the lipophilic tails. Poly(ethylene glycol) (PEG_{2000} MW = 2000) was chosen because of its size and the well-known empathy for water. The presence of long chains exposed on the surface of the aggregates, such as those obtained using high-molecular-weight PEG as spacer, prevents them from being cleared through the reticulo-endothelial system (RES).[18] Furthermore it also avoids adsorption of blood proteins onto the supramolecular surface and, thus, the protective capacity of the PEG corona is of primary importance for the in vivo use of the supramolecular aggregates.[19] The bifunctional chelating agent, a DTPA derivative, is bound on the lipophilic moiety of the other monomer. It was chosen for its ability to give stable complexes with different metals such as the radioactive metals used for diagnostic or therapeutic nuclear medicine applications, thus allowing the in vivo visualization of the nanovectors.[20] The ability of the new aggregates to act as target selective nanovectors is demonstrated in vitro and in vivo; moreover a preliminary study concerning the drug loading capability and the drug activity on target cells, using the well-known cytotoxic drug Doxorubicin, is reported.

Results and Discussion

The knowledge of the structural parameters (shape and size) of the aggregates is a crucial step in the development of nanocarriers for drug delivery. The aggregate dimension and their nature (spherical or rod-like micelles, vesicles, or liposomes) could determine the in vivo stability and biodistribution of the nanocarriers, and the rate of drug release.[21] Moreover the selective binding of the peptide containing nanocarriers to the target receptor site is only possible if the bioactive peptide sequence is well-exposed on the aggregate's external surface, thus enhancing the probability for an effective homing of nanovectors on the selected target.

We have already reported that the structure obtained by self-assembling anionic surfactants such as $(C18)_2$DTPAGlu can be influenced by several parameters such as pH, temperature, ionic strength of the medium, and chemical composition of the solvent.[22] Moreover, when a second nonionic monomer is introduced in the aggregate a structural transition can occur. In the mixed aggregates the molar ratio between the two monomers plays a crucial role in the assembly process.[15] In this study we fixed pH at physiological levels (pH 7.4), and the molar ratio between the monomers ($(C18)_2$DTPAGlu/$(C18)_2PEG_{2000}$CCK8) at 70:30). To characterize the supramolecular aggregates obtained by mixing the two synthetic monomers, a fully structural characterization was carried out by using several physicochemical techniques.

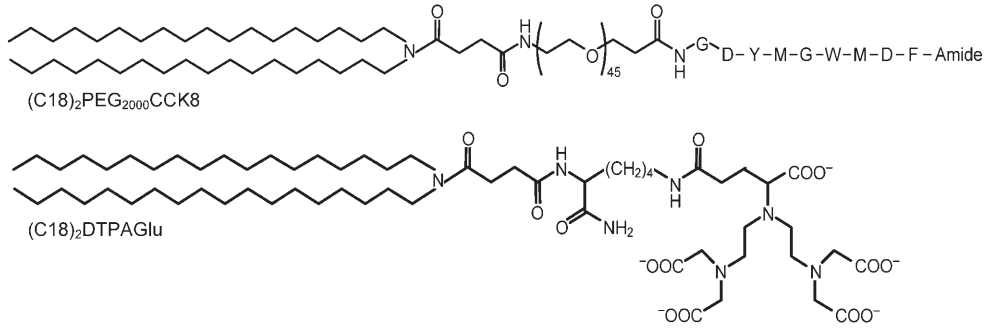

Figure 1. Schematic representation of the two monomers ($(C18)_2PEG_{2000}$CCK8 and $(C18)_2$DTPAGlu) employed to formulate mixed aggregates.

Structural characterization

Structural characterization has been performed on the supramolecular aggregates that appear very stable: they present very low cmc values: 1.8×10^{-6} M for the self-assembled $(C18)_2PEG_{2000}CCK8$ and 2.1×10^{-6} M for the mixed aggregate $(C18)_2DTPAGlu/(C18)_2PEG_{2000}CCK8$.

Microstructural parameters of the aggregates present in solution as well as the presence of possible a coexisting population of aggregates differing in size and shape have been obtained by light and neutron scattering techniques (DLS and SANS) and cryogenic transmission electron microscopy (Cryo-TEM). The DLS relaxation time distributions are monomodal at all angles studied, with a very broad peak that suggests the co-presence in solution of a wide spread of aggregates, see Figure 2a. The linear relation of the relaxation rate as a function of q^2 confirms that the mode is due to translational diffusion processes, attributed to a complex with apparent translational diffusion coefficient $D=(1.66\pm0.01)\times10^{-12}$ m^{2}s. This data can be directly related to the hydrodynamic radius of the aggregate, R_H, through the Stokes-Einstein equation:

$$R_H = \frac{k_B T}{6\pi\eta D} \quad (1)$$

where k_B is the Boltzmann constant, T is the absolute temperature, and η is the medium viscosity. The value obtained for the hydrodynamic radius was of about 120 ± 10 Å.

The above results were confirmed by the SANS measurements. In fact the scattering cross section $d\Sigma/d\Omega$, reported in Figure 2b shows a q^{-2} decay at low q values, which is typical of bilayer scattering (open bilayers and/or closed vesicles) and a q^{-1} decay in the intermediate q range as expected in the presence of rod-like micelles.[23]

In all cases, the supramolecular aggregates appear to contain both monomers as suggested by a considerable increase in scattering cross section observed in samples obtained with the addition of the $(C18)_2PEG_{2000}CCK8$ monomer with respect to the already reported self-assembling obtained by $(C18)_2$DTPAGlu amphiphile.[22] The observed increase reflects the additional contribution to the scattering cross section, due to the presence of $(C18)_2PEG_{2000}CCK8$ in these aggregates.[24]

The structural parameters of the aggregates have been obtained using the models as reported in the experimental section, and are summarized in Table 1.

The analysis of the bilayer structure (thickness ~65 Å, length ~800–1000 Å) and the length of poly(ethylene glycol) spacer suggest that the bioactive peptide is completely exposed on the external surface of the aggregates and available for receptor binding. In fact according to the crystallographic data, the length of the PEG_{2000}, present in the shell, should be around 30 Å,[25] that is, quite larger than the polar heads exposed by $(C18)_2$DTPAGlu monomers on

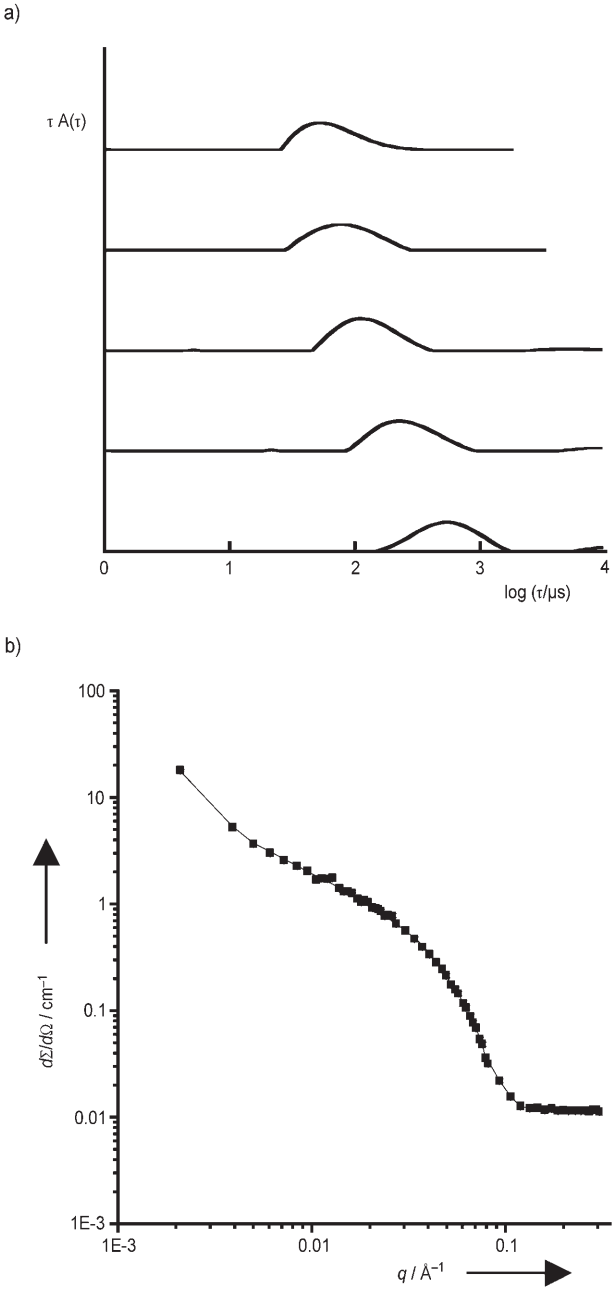

Figure 2. a) Relaxation time distributions at θ 45°–120° for $(C18)_2$DTPAGlu-$(C18)_2PEG_{2000}$-CCK8 (70:30) aqueous solution at pH 7.4. b) Experimental small-angle neutron scattering data collected on $(C18)_2$DTPAGlu-$(C18)_2PEG_{2000}CCK8$ (70:30 molar ratio) mixed aggregates. Fitting of the data according to the respective model gives the solid lines shown for the two samples.

Table 1. Summary of structural parameters obtained by SANS and DLS techniques.

System	R [Å][a]	l [Å][a]	d [Å][b]	D [10^{12} m^{2}s^{-1}][c]	R_H [Å][c]
$(C18)_2$DTPAGlu-$(C18)_2PEG_{2000}CCK8$-water	37 ± 3	700 ± 20	65 ± 9	1.66 ± 0.01	120 ± 20

[a] R and l are radius and length of rod-like micelles. [b] d is the thickness of double bilayers. [c] D and R_H are diffusion coefficient and hydrodynamic radius of the aggregates as measured by DLS.

the hydrophilic shell (~20 Å). The same arguments hold in the case of rod-like micelles whose radius is ~40 Å and length is above 700 Å. The total number of monomers in $(C18)_2$DTPAGlu/$(C18)_2PEG_{2000}$CCK8 mixed aggregates is expected to be above 200 for the rod-like micelles and $\sim 2\times10^5$ for bilayers. In all aggregates there is a large water penetration, due to the steric repulsion among the charged DTPAGlu heads.

The cryo-TEM image reported in Figure 3 shows the presence of hollow tubes that can correspond to open bilayers structures, whereas vesicles have not been detected.

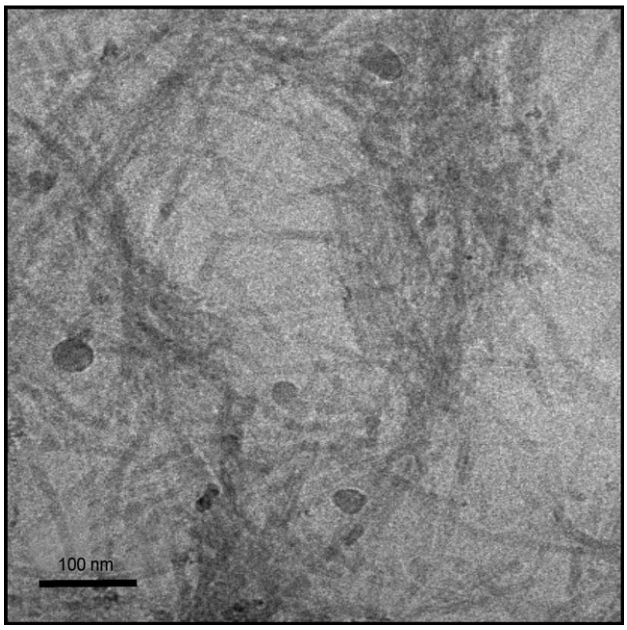

Figure 3. Cryo-TEM image of mixed aggregates formed by $(C18)_2$DTPAGlu and $(C18)_2PEG_{2000}$CCK8. Circular spots are artifacts.

Thus, in the experimental conditions we investigated, there is the presence of polydisperse kinds of aggregates, such as rod-like micelles, bilayer fragments, and probably vesicles, in solution as the broad peak obtained by DLS suggests. In the already reported $(C18)_2$DTPAGlu self-assembling system[22] the relaxation time distribution at physiological pH revealed the contemporary presence of micelles and bilayer structures or vesicles and that the dominant aggregates present in the system were micelles. The micelle formation is explained by the high negative charge of the surfactant head group, which causes strong head group–head group interactions. In the mixed system, described herein, the $(C18)_2PEG_{2000}$CCK8 nonionic monomer interposes among $(C18)_2$DTPAGlu units, partially shielding the electrostatic repulsions between the chelating agent polar heads and promoting the formation of bilayers.

In vitro biological assays

As already reported for other mixed aggregate systems,[15] receptor binding ability can be evaluated by standard nuclear medicine experiments. Radiolabeling of the aggregates was performed at concentrations above critical micellar concentration to avoid the presence of free monomers in solution. Trace amounts of $^{111}InCl_3$ and up to 500 μCi were added to the aggregate formulation after addition of an equal volume of 0.5 N Sodium Citrate. Confirmation of incorporation of the label into the aggregates was obtained by gel filtration. ^{111}In-labeled aggregates showed preferential binding to A431 cells overexpressing the CCK_2-R by transfection (Figure 4a) compared to control cells. As a certain degree of nonspecific binding and internalization of the aggregates was expected, experiments were performed both at 4 °C (to block cellular metabolic processes such as nonspecific internalization) and at 37 °C (to keep metabolic processes active). Specific targeting on receptor expressing cells was demonstrated as these cells showed significantly higher retention of label compared to control cells. Although these differences were fairly small they were confirmed by performing competition experiments with excess unlabeled free CCK8 peptide that displaced all specifically bound aggregate to background levels. No significant differences in accumulation on receptor positive cells was observed between cells incubated at 37 °C and 4 °C for the incubation time (1 h) tested, indicating little, if any, internalization during the short observation period of the experiment. Although uptake levels overall were fairly low, receptor targeting both at 37 and 4 °C allowed a several-fold increase in cell associated activity on A431-CCK_2-R cells compared to controls.

In vivo binding and biodistribution studies

^{111}In-labeled aggregates were also used to determine in vivo properties of the nanovectors and their ability to target in vivo receptor positive tumor with respect to control tumor. Results of the biodistribution experiments at 18 h are shown in Figure 4b. Overall retention of the radiolabel in the experimental animals was very high, with essentially no excretion of the starting radioactivity over the observation period. Biodistribution of the labeled aggregates is consistent with a fairly low plasma clearance. All organs showed high retention of radioactivity although this was particularly evident in organs with high blood pool such as liver and spleen. There was higher concentration of the aggregates in the receptor expressing xenografts. Direct comparisons of tumor uptake within the same animal showed statistically significant enrichment of the aggregates in the receptor expressing xenografts (Paired t-test, $P=0.01$) compared to control. The average enrichment factor was found to be 48 ± 21% (mean $\pm$SD, percent increase of weight normalized radioactivity in receptor positive versus radioactivity in receptor negative tumors, corrected for radioactivity present in blood and interstitial space of the tumor).[26]

To maintain the aggregates stable, high concentration of the monomers was used to stay above the critical micellar concentration. Surfactants (2 mg in 100 μL of solution) were injected in each animal. Although milligram quantities of aggregates were injected, we did not observe any significant side effect following the i.v. administration of the compound and during the 18 h observation period.

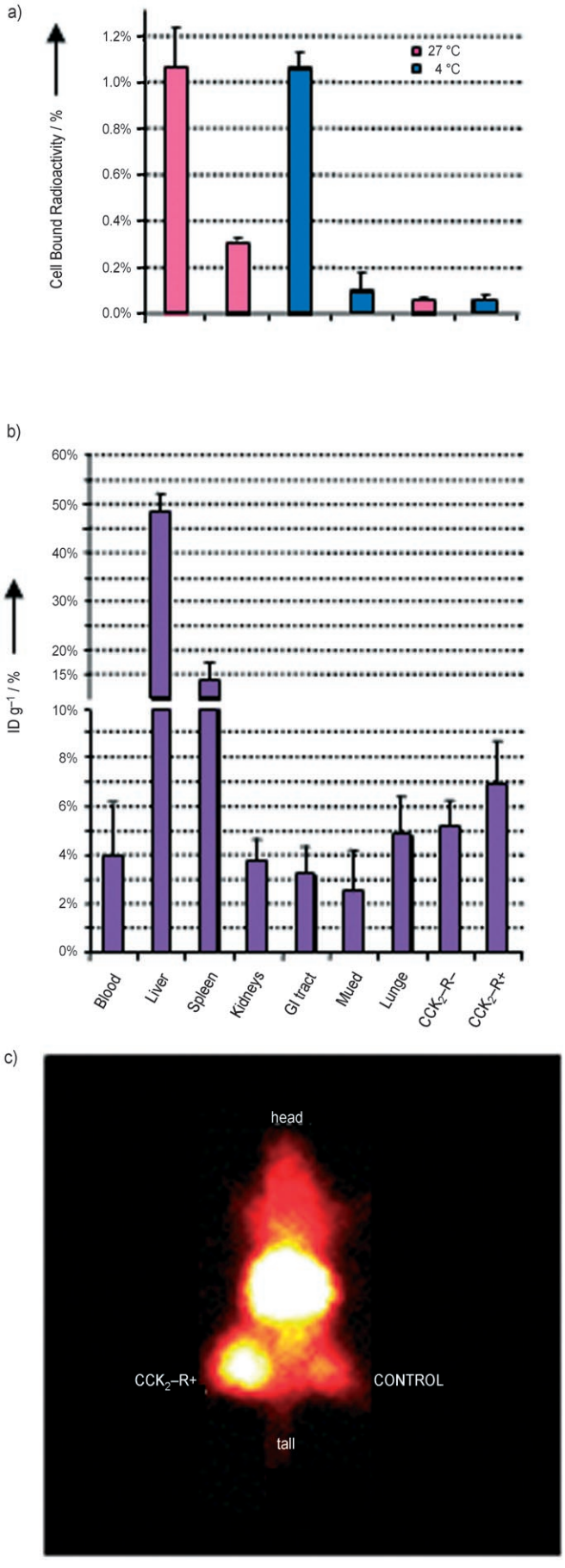

Figure 4c shows the gamma camera image of a mouse from the biodistribution experiment taken prior to dissection. The image clearly shows increased accumulation of the radiolabeled aggregates in the receptor positive xenograft compared to surrounding tissues and the contralateral control tumor. Very high retention was also observed in liver and spleen, two high blood pool organs. The receptor positive tumor clearly stands out compared to the background activity that is fairly uniform and high in the remaining organs, in agreement with the data obtained from the cut-up experiments. All the injected radioactivity is recovered from the animals after 18 h. This indicates that the aggregates have fairly long circulating half-life and very little clearance through digestive or urinary tract. The elevated concentrations in high blood pool organs and the considerable ability to concentrate in the receptor expressing xenografts are all in line with desired and necessary pharmacokinetic properties of a drug delivery nanovector.

Doxorubicin loading and in vitro assays

Doxorubicin was loaded in the hydrophobic core of the rod-like micelles and open bilayers by hydrating the lipid film for 30 min with a solution of doxorubicin buffered at pH 7.4. The phosphate buffer was diluted at 0.01 M (instead 0.1 M used for the physicochemical characterization) because of the poor solubility of doxorubicin in phosphate solution over the range of pH 5.0–8.5.[27] The doxorubicin loading content was calculated by fluorescence measurements for subtraction of the amount of free doxorubicin, eluted by gel filtration, from the total amount of loaded doxorubicin.[28] The high value of doxorubicin loading content (DLC higher than 99% of the total) allows the use of the doxorubicin containing aggregates as obtained. The amount of doxorubicin molecules per aggregate (2:1) was calculated taking into account the aggregation number (about 200 monomers per micelle). These amounts do not represent the doxorubicin loading efficiency of the aggregates or the upper limit of loading, but the ratio chosen for the experiments. Cytotoxicity studies were carried out by a cell growth inhibition assay. Cells were treated for 16 h with aggregates containing doxorubicin at different final doxorubicin concentrations, ranging between 20 and 200 ng mL^{-1}, and then incubated for another four days after which cell survival was assessed using a sulforhodamine B assay.[29] Control experiments performed with increasing concentrations of the empty aggregates showed no significant killing effect in both cell systems at concentrations of monomer up to 500 ng mL^{-1}. Data were

Figure 4. Biological characterization of radiolabeled nanovectors. a) Binding of ^{111}In-labeled aggregates to A431 cells overexpressing the CCK_2-R by transfection compared to control cells. Binding is measured at two different temperatures, 4 and 37 °C. b) Biodistribution results of experiments performed in receptor positive and receptor negative xenografts bearing nude mice 18 h after injection. Organs with high blood pool such as liver and spleen displayed highest activity retention levels. c) Gamma camera image (dorsal view) obtained prior to dissection of one of the animals 18 h after injection of radiolabeled aggregates clearly shows higher concentration of the radiolabel in the receptor positive xenograft (+, left flank) compared to the control tumor (−, right flank). These differences were statistically significant when comparing data from the five animals (paired t-test, $P = 0.01$).

plotted as the percentage of surviving cells compared to the control cells. Incubation of receptor-positive and control cells (Figure 5) showed significantly lower cell survival in receptor-expressing cells for samples incubated in the presence of the higher amounts of doxorubicin (final concentrations of 100 and 200 ng mL^{-1}). Lower concentrations of the drug containing aggregates (not shown) showed a lower overall killing effect and no significant differences between receptor positive and receptor negative cells.

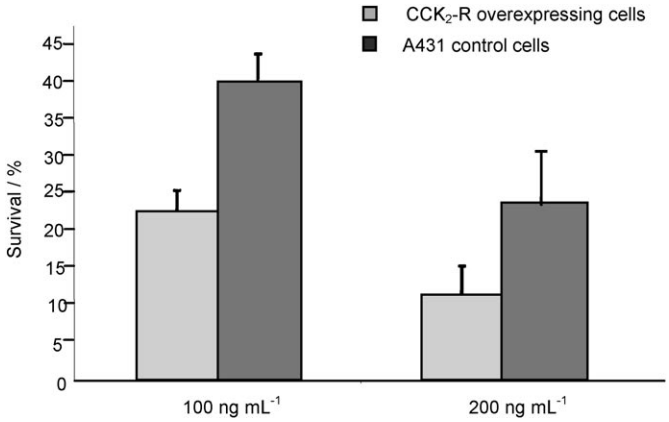

Figure 5. Cell survival assays of CCK_2-R overexpressing and control A431 cells incubated with different amounts of doxorubicin containing vesicles for 16 h then followed for four further days. A receptor specific effect is observed in cells incubated with high concentrations of doxorubicin. No receptor specificity was observed at the lower concentrations although some cell killing effect was evident in both cell lines.

These preliminary findings indicate that specific interaction of the peptide-containing aggregates with their receptor indeed increases the therapeutic efficacy of the doxorubicin containing aggregates. At lower concentrations receptor specific killing is not observed likely due to lower receptor occupancy secondary to dilution of the aggregates. In preliminary experiments performed with doxorubicin alone under the same conditions higher cell killing was observed for the same concentrations and no differences between the receptor expressing and nonexpressing cell lines (data not shown), suggesting that when doxorubicin is loaded into the aggregates its toxicity is significantly reduced probably because the drug is not as readily available to enter the cells as when placed directly in the culture medium.

Conclusions

In conclusion, under the experimental conditions we investigated, the monomers described herein form a variety of aggregates of different shapes and sizes: rod-like micelles with a radius of ~40 Å and length above 700 Å, bilayer fragments with thickness ~65 Å, and probably vesicles. Notwithstanding the high polydisperse kind aggregates, biological tests show properties that appear potentially suitable for clinical applications: 1) significantly higher concentration of aggregates in receptor expressing xenografts relative to controls has been established in vivo, suggesting that these aggregates may be used to increase concentration of a therapeutic or diagnostic agent to tissues expressing a specific receptor target; 2) slow plasma kinetics with prolonged half-life and low breakdown of the supramolecular aggregates, both probably due to the presence of PEG_{2000} moieties on the aggregate external surface,[18,19] appear useful for maintaining high blood concentrations of the desired agent.

The ability of surface exposed peptides to target nanovectors to a specific organ/tissue gives promising new opportunities for the development of pharmaceutical agents with higher selectivity toward a biological target and may potentially reduce toxic side effects on nontarget organs. In particular these aggregates, the use of which we are evaluating, appear to increase delivery of doxorubicin to receptor-positive cells as confirmed by the increased killing effect obtained in these cells compared to nonreceptor expressing controls.

Experimental Section

Materials and methods

Protected N^{α}-Fmoc amino acid derivatives, coupling reagents, and Rink amide MBHA resin were purchased from Calbiochem-Novabiochem (Laufelfingen, Switzerland). Fmoc-NH-PEG2000-NHS (MW = 2384 Da) was purchased from Nektar therapeutics (Huntsville, AL). All other chemicals were commercially available by Sigma–Aldrich or Fluka (Bucks, Switzerland) or LabScan (Stillorgan, Dublin, Ireland) and were used as received unless otherwise stated. *N*,*N*-dioctadecylsuccinamic acid was synthesized according to the literature.[30] All solutions were prepared by weight with doubly distilled water. Samples to be measured by Small Angle Neutron Scattering (SANS) techniques were prepared using heavy water (Sigma–Aldrich, purity > 99.8%). The pH of all solutions was kept constant at 7.4. Doxorubicin HCl, (commercial name of (8*S*,10*S*)-10-(4-amino-5-hydroxy-6-methyl-tetrahydro-2H-pyran-2-yloxy)-6,8,11-trihydroxy-8-(2-hydroxyacetyl)-1-methoxy-7,8,9,10-tetrahydro-tetracene-5,12-dione) was purchased from Sigma–Aldrich.

Preparation of $(C_{18}H_{37})_2NCO(CH_2)_2COLys(DTPAGlu)CONH_2$ ($(C18)_2DTPAGlu$)

The synthesis of $(C_{18}H_{37})_2NCO(CH_2)_2COLys(DTPAGlu)CONH_2$ monomer was carried out as previously described.[22]

Preparation of $(C_{18}H_{37})_2$-$NCO(CH_2)_2CO$-PEG_{2000}-G-CCK8 ($(C18)_2PEG_{2000}CCK8$)

Synthesis of the $(C_{18}H_{37})_2$-$NCO(CH_2)_2CO$-PEG_{2000}-G-CCK8 monomer was carried out in solid-phase using a 433A Applied Biosystems automatic synthesizer under standard conditions and Fmoc strategy.[31] Rink-amide MBHA resin (0.78 mmol g^{-1}, 1.0 mmol scale, 1.28 g) was used. The peptide chain was elongated by sequential coupling and Fmoc deprotection of the following Fmoc-amino acid derivative: Fmoc-Phe-OH, Fmoc-Asp(O*t*Bu)-OH, Fmoc-Met-OH, Fmoc-Trp(Boc)-OH, Fmoc-Gly-OH, Fmoc-Met-OH, Fmoc-Tyr(*t*Bu)-OH, Fmoc-Asp(O*t*Bu)-OH, Fmoc-Gly-OH. All couplings were performed twice for 1 h, by using an excess of four equivalents for the single amino acid derivative. The α-amino acids were activated in situ by the standard conditions by using hydroxybenzotriazole/benzotria-

zol-1-yloxytris(pyrrolidino) phosphonium/*N*,*N*-diisopropylethylamine (HOBt/PyBop/DIPEA) procedure. *N*,*N*-dimethylformamide (DMF) was used as a solvent. Fmoc deprotection was carried out by 20% solution of piperidine in DMF after the coupling of each amino acid residue. The coupling steps were monitored by the qualitative Kaiser test. When the peptidic synthesis was complete, the Fmoc N-terminal protecting group was removed and Fmoc-NH-PEG_{2000}-NHS residue condensed. The coupling was performed in DMF twice for 1 h, by using an excess of 1.5 equivalents and 3.0 equiv of DIPEA. The coupling reaction was monitored by the qualitative Kaiser test. Fmoc deprotection was carrier out by 20% solution of piperidine in DMF. Than, *N*,*N*-dioctadecylsuccinamic acid was bonded on the α-NH_2 of PEG_{2000} hydroxy spacer. The coupling was carried out by an excess of four equivalents (0.622 g, 1 mmol) of the lipophilic compound dissolved in 3 mL of *N*,*N*-dimethylformamide/dichloromethane/*N*-methylpyrrolidone DMF/DCM/NMP (1:1:1) mixture. PyBop (0.520 g, 1.0 mmol), HOBt (0.153 g, 1.0 mmol), and DIPEA (335 μL, 2.0 mmol), dissolved in DMF were introduced in the vessel like activating agents. The coupling time was 1 h under N_2 flow at room temperature. The monomer-resin was treated with an acidic solution of trifluoroacetic acid/triisopropylsilane/water TFA/TIS/H_2O (95.5:2.0:2.5) mixture. The crude product was precipitated at 0 °C by adding water dropwise. Purification of the crude mixture was carried out by RP-HPLC using a Waters model Delta Prep 4000 chromatograph. Product was analyzed for purity by Shimadzu 10A-LC HPLC equipped with a Phenomenex C_{18} column and for identity by ESI-MS using a Finnigan Surveyor MSQ single quadrupole electrospray ionization mass spectrometer (Finnigan/Thermo Electron Corporation San Jose). Analytical RP-HPLC indicated a purity >95%. *(C18)$_2$PEG$_{2000}$CCK8*, $R_t = 27.1$ min; $M_W = 3774$ amu; $[M + 3H^+]/3 = 1259.0$ amu

Sample preparation

All solutions were prepared by weight, buffering the samples at pH 7.4 by using 0,1 M phosphate buffer. pH was controlled by using pH-meter MeterLab PHM 220. In most cases the samples to be measured were prepared from stock solutions. Aggregates were prepared by dissolving the amphiphiles, in the molar ratio $(C18)_2$DTPAGlu/$(C18)_2PEG_{2000}$CCK8) 70:30, in a small amount of a methanol/chloroform (50:50) mixture, and subsequently evaporating the solvent by slowly rotating the tube containing the solution under a stream of nitrogen. In this way a slowly formed thin film of amphiphile was obtained. After leaving the film under reduced pressure for several hours, the organic solvent was evaporated. Then the film was hydrated by addition of 0.1 M phosphate buffer (pH 7.4) solution in the vial and stirred for 1 h by vortex. The product was successively subjected to sonication for 1 h, and finally extruded pushing the solution ten times through a polycarbonate membrane with 100 nm pore size. Extrusion procedure was performed by using the Avanti Mini extruder available by Avanti Polar Lipids (USA and Canada).

Small-angle neutron scattering (SANS)

Small-angle neutron scattering measurements performed at Neutron facilities Berlin Neutron Scattering Centre, Hahn-Meitner-Institute, Berlin, Germany. Neutrons with an average wavelength λ of 7 Å and a wavelength spread $\Delta\lambda/\lambda < 0.1$ were used. The configurations adopted allowed collection of the scattering cross section in an interval of transferred moment q ranging, depending on the facilities, between 0.001 and 0.12 $Å^{-1}$. The measurement time ranged between 30 min and 2 h per sample. The raw data, obtained by studied samples were then corrected for electronic background and empty cell scattering. Detector efficiency corrections and transformation to absolute scattering cross sections were made with appropriate standards, according to standard procedures. Microstructural parameters of the aggregates have been obtained applying the appropriate models to the experimental SANS data.

Provided the analyzed solutions are quite dilute, consequent structure function $S(q)$ can be approximated to the unity, and the scattering cross section $d\Sigma/d\Omega$ of a collection of monodisperse bodies can be described by the following equation[32]

$$\frac{d\Sigma}{d\Omega} = N_b P(q) + \left(\frac{d\Sigma}{d\Omega}\right)_{inch} \quad (2)$$

where N_b is the number density of scattering bodies, $P(q)$ is the form factor containing information on the shape of the scattering objects, and $(d\Sigma/d\Omega)_{inch}$ is the incoherent contribution to the total scattering cross section, mainly due to the presence of hydrogen nuclei in the sample, that can be evaluated. Micelles and vesicles resulting from the aggregation processes may assume different shapes like rods, platelets, spheres, and so on. Scattering from a cylindrical or rod-like structure is characterized by a linear portion in a Porod (double log) plot of $d\Sigma/d\Omega$ vs. q with a slope of -1. Using the Guinier approximation,[33] cross section for such aggregates can be written as

$$\frac{d\Sigma}{d\Omega} = \phi(1-\phi)\frac{(\pi R \Delta\rho)^2}{q}\exp\left(-\frac{q^2R^2}{4}\right) \quad (3)$$

where Ψ is the volume fraction of the cylinders, R their radius, ΔP representing the contrast between the cylinders and the solvent (D_2O). By plotting $\ln(q\ d\Sigma/d\Omega)$ versus q from the linear portion is possible to extract the radius R of cylinders. A lower limit for cylinders length can be obtained analyzing the Guinier region of the scattering cross section since for $d > 2\pi/q$ the pattern presents a flattening typical of this region. Scattering from planar structures is characterized by a linear portion in a Porod plot of $d\Sigma/d\Omega$ vs. q with a slope of -2. In the q range analyzed vesicles can be "approximated" as bilayer, so the factor structure used is that one for a planar sheet,[34] given by

$$\frac{d\Sigma}{d\Omega} = 2\pi(\Delta\rho)^2 S\tau^2 \frac{1}{q^2}\frac{\sin^2\left(\frac{q\tau}{2}\right)}{\left(\frac{q\tau}{2}\right)^2} \quad (4)$$

where τ is the bilayer's thickness and S is the plain surface per volume.

Dynamic light scattering (DLS)

The setup for the dynamic light scattering measurement was an ALV/DLS/SLS-5000F, CGF-8F based compact goniometer system from ALV-GmbH., Langen, Germany. The light source was constituted by a CW diode-pumped Nd: YAG solid-state Compass-DPSS laser with a symmetrizer from COHERENT, Inc., (Santa Clara, California). It operated at 532 nm with a fixed output power of 400 mW. The laser intensity could be modulated by an external compensated attenuator from Newport Inc., USA. A more detailed description of the instrumentation can be found in the literature with the difference that decalin was used instead of toluene as a refractive index matching liquid.[35] The DLS data were analyzed by nonlinear regression procedures. The models used in the fitting procedures are expressed with respect to the normalized time correlation function of the electric field, $g^{(1)}$ (t), whereas the fitting was performed directly to the experimentally measured time correlation function

of the scattered intensity G(2)(t) often presented as the normalized function, $g^{(2)}(t)-1$,[36] and described by the Siegert relation[37,38]

$$g^{(2)}(t) - 1 = \beta\left|g^{(1)}(t)\right|^2 \quad (5)$$

where β ($\leq$ 1) is a no ideality factor, which accounts for deviation from ideal correlation and depends on the experimental geometry. $g^{(1)}$ (t) can either be a single-exponential or multiexponential decay with corresponding relaxation times, τ, depending on the system investigated. It can be written as the Laplace transform of the distribution of relaxation time, $A(\tau)$:

$$g^{(2)}(t) = \int_{-\infty}^{+\infty} \tau A(\tau) \exp\left(-\frac{t}{\tau}\right) d\ln\tau \quad (6)$$

where $\tau = \Gamma^{-1}$, whereas Γ is the relaxation rate that is used to calculate the diffusion coefficient D. The relaxation time distribution $\tau A(\tau)$ is obtained by regularized inverse Laplace transformation (RILT) of the measured intensity correlation function using calculation algorithms REPES, as incorporated in the GENDIST analysis package.[38–40] The relaxation rate Γ is obtained from the first moment of the relaxation time distribution, and from its value the apparent translational diffusion coefficient D is estimated, by this relation

$$D = \lim_{q\to 0} \frac{\Gamma}{q^2} \quad (7)$$

Where q is the absolute value of the scattering vector ($q = 4\pi\, n_0 \sin(\theta/2)/\lambda$), where n_0 is the refractive index of the solvent, λ is the incident wavelength, and θ is the scattering angle. Thus D is obtained from the slope of Γ as a function of q^2, where Γ is measured at different scattering angles (θ) ranging from 45° to 120°. The corresponding relaxation time distributions [$\tau A(\tau)$ versus $\log(\tau/\mu s)$], obtained by regularized inverse Laplace transformation of the correlation functions, are presented in Figure 2a.

Cryogenic transmission electronic microscopy (Cryo-TEM)

Cryo-TEM images were carried out at the Chemical Centre of Lund, Sweden on a Philips 120 Biotwin microscope operating at 120 kV. A small drop of the sample solution was applied on a copper EM grid with a holey carbon film, and excess solution was blotted with a filter paper, leaving thus a thin sample film spanning the holes in the carbon film. The film was subsequently vitrified at the desired temperature by quick freezing in liquid ethane and analyzed in the microscope at about −170 °C. Sample preparation was carried out in a controlled environment verification system to avoid water evaporation and to ensure cryofixation of the specimen at a controlled temperature (25 °C).[41]

Biological assays

Radiolabeling of the aggregates was performed at concentrations of the monomers above $8.0\cdot10^{-3}$ M. Trace amounts of $^{111}InCl_3$ and up to 500 μCi were added to the aggregate formulation after addition of an equal volume of 0.5 N Sodium Citrate. Confirmation of incorporation of the label into the aggregates was obtained by gel filtration on Sephadex G-50 prepacked columns (Pharmacia Biotech). Binding activity was tested on A431 cells overexpressing the CCK_2-R by stable transfection[29] and compared to control cells. Assays were performed at 4 and 37 °C on cell suspensions that were incubated with the radiolabel aggregates for 1 h in the presence (100-fold excess with respect to CCK8 K_d) or absence of excess CCK8 peptide. Concentration of the monomers in the cell binding assays were always kept above 10^{-4} M. Radioactivity bound to cells was separated from unbound activity by centrifugation through dibutyl phthalate in 1.5 mL tubes which were subsequently frozen on dry ice, the cell pellet containing portion of the tube excised and counted in a Wallac gamma counter. Unbound radioactivity was placed in a separate vial and counted as well. Experiments were performed in triplicate and the percentage of bound radioactivity determined under the different experimental conditions.

In vivo experiments

Animal experiments were carried out on six week old female CD1 nude mice (Charles River Italia) in whom subcutaneous xenografts of A431-CCK_2-R overexpressing and control A431 cells were grown in opposite flanks as previously described.[29] Procedures involving animals and their care were in conformity with institutional guidelines that comply with national and international laws and policies. Biodistribution and imaging experiments were performed two weeks after implanting cells (tumor sizes were between 0.5 and 1 g). Approximately 100 μCi of ^{111}In-labeled aggregate preparation were injected into the lateral tail vein of each mouse ($n = 5$). Imaging was performed at different times after injection, following administration of an intraperitoneal anesthetic on a clinical gamma camera equipped with a medium energy collimator. Eighteen hours after injection the mice were killed, imaged, and subsequently dissected to quantitatively determine organ concentrations of radioactivity by weighing and counting each dissected organ. The results were expressed as percentage of the injected dose g^{-1} normalized to a 20 g mouse. Direct comparisons were also performed in each mouse between the receptor positive and receptor negative xenografts.

Loading of doxorubicin into aggregates

A mixture of $(C18)_2$DTPAGlu, 8 mg, and of $(C18)_2PEG_{2000}$CCK8, 12 mg, (molar ratio 70:30) was dissolved in 2 mL of MeOH/$CHCl_3$ (50:50). After stirring, the organic solvents were removed under a slow nitrogen flow and a lipid film was obtained. The lipid film was hydrated for 30 min by using 10.0 mL of a Doxorubicin solution (concentration 10 μg mL^{-1}) in 0.01 M phosphate buffer at pH 7.4. Doxorubicin concentration, in all experiments, was determined by spectroscopic measurements (UV or fluorescence) using calibration curves obtained by measuring absorbance at 480 nm or fluorescence emission at 590 nm for several solutions containing different amounts of free doxorubicin in 0.01 M phosphate buffer (pH 7.4). UV spectra were obtained on a UV-vis Jasco (Easton, MD) Model 440 spectrophotometer with a path length of 1 cm; fluorescence spectra were recorded on a Jasco Model FP-750 spectrofluorimeter by using 1.0 cm path length quartz cell. Emission spectra were recorded at room temperature. Equal excitation and emission bandwidths were used throughout experiments, with a recording speed of 125 nm min^{-1} and automatic selection of the time constant. Free Doxorubicin was removed by using a Sephadex G50 column pre-equilibrated with 0.1 M phosphate buffer at pH 7.4. All fractions (150 μL) were collected in eppendorf and analyzed by fluorescence spectroscopy to determine the amount of free Doxorubicin. The Doxorubicin-loading content (DLC, defined as the weight percentage of Doxorubicin in the aggregates) was quantified for subtraction of the amount of Doxorubicin removed from the column from the total amount of Doxorubicin loaded.

Cell survival assays

The A431 cells overexpressing the CCK_2 receptor and control cells described above were used to assess biological properties of the drug containing aggregates. Cells were seeded at a density of 1000 cells per well in 96-well plates. The following day a suspension of the Doxorubicin containing aggregates was added to triplicate wells of control and CCK_2-R expressing cells. The overall volume of medium in each well was kept constant, and the final concentration of doxorubicin on the cells ranged from 20 to 200 ng mL^{-1}. Control experiments, on both cell lines, were performed using increasing amounts of empty aggregates ranging from 10 to 500 ng mL^{-1}. Cells were maintained for approximately 16 h in the presence of the aggregates after which the solution was removed and fresh medium was added to each well. Cells were then incubated for an additional four days to assess cell survival which was performed using the well-established colorimetric sulforhodamine B assay.[42] Data were plotted as the percentage of surviving cells compared to untreated cells.

Acknowledgements

The authors thank the European Molecular Imaging Laboratories Network (EMIL) for financial support. We thank Prof. Olle Söderman for the insightful discussion, Mrs. Gunnel Karlsson for the technical assistance for cryo-TEM image and Dr. Luigi Del Pozzo for experimental assistance. Authors thank Astrid Brandt at Hahn-Meitner Institut, Berlin, for the provision of beam-time for measurements with neutrons. SANS experiments have been supported by the European Commission, NMI3 Contract RII3-CT-2003-505925.

Keywords: CCK8 peptide · drug delivery · dynamic light scattering · small angle neutron scattering · supramolecular aggregates

[1] R. Langer, *Nature* **1998**, *392*, 5–10.
[2] V. P. Torchilin, *Nat. Rev. Drug Discovery* **2005**, *4*, 145–160.
[3] V. P. Torchilin, *J. Controlled Release* **2001**, *73*, 137–172.
[4] M. Ferrari, *Nat. Rev. Cancer* **2005**, *5*, 161–17.
[5] M. T. Allen, *Nat. Rev. Cancer* **2002**, *2*, 750–763.
[6] E. D. Lobo, R. J. Hansen, J. P. Balthasar, *J. Pharm. Sci.* **2004**, *93*, 2645–2668.
[7] L. Aloj, G. Morelli, *Curr. Pharm. Des.* **2004**, *10*, 3009–3031.
[8] D. Kwekkeboom, E. P. Krenning, M. De Jong, *J. Nucl. Med.* **2000**, *41*, 1704–1713.
[9] S. W. Lamberts, E. P. Krenning, J. C. Reubi, *Endocr. Rev.* **1991**, *12*, 450–482.
[10] V. P. Torchilin, *Cell. Mol. Life Sci.* **2004**, *61*, 2549–2559.
[11] W. J. M. Mulder, G. J. Strijkers, G. A. F. van Tilborg, A. W. Griffioen, K. Nicolay, *NMR Biomed.* **2006**, *19*, 142–164.
[12] W. J. M. Mulder, G. J. Strijkers, A. W. Griffioen, L. van Bloois, G. Molema, G. Storm, A. Koning, K. Nicolay, *Bioconjugate Chem.* **2004**, *15*, 799–806.
[13] A. Accardo, D. Tesauro, P. Roscigno, E. Gianolio, L. Paduano, G. D'Errico, C. Pedone, G. Morelli, *J. Am. Chem. Soc.* **2004**, *126*, 3097–3107.
[14] A. Accardo, D. Tesauro, G. Morelli, E. Gianolio, S. Aime, M. Vaccaro, G. Mangiapia, L. Paduano, K. Schillén, *J. Biol. Inorg. Chem.* **2007**, *12*, 267–276.
[15] D. Tesauro, A. Accardo, E. Gianolio, L. Paduano, J. Texeira, K. Schillén, S. Aime, G. Morelli, *ChemBioChem* **2007**, *8*, 950–955.
[16] D. F. Mierke, C. Giragossian, *Med. Res. Rev.* **2001**, *21*, 450–471.
[17] J. C. Reubi, J. C. Schaer, B. Waser, *Cancer Res.* **1997**, *57*, 1377–1386.
[18] V. P. Torchilin, V. G. Omelyanenko, M. I. Papisov, A. J. Bogdanov, V. S. Trubetskoy, J. N. Herron, C. A. Gentry, *Biochim. Biophys. Acta Biomembr.* **1994**, *1195*, 11–20.
[19] V. S. Trubetskoy, V. P. Torchilin, *Adv. Drug Delivery Rev.* **1995**, *16*, 311–320.
[20] S. Liu, D. S. Edwards, *Bioconjugate Chem.* **2001**, *12*, 7–34.
[21] S. M. Moghimi, A. C. Hunter, J. C. Murray, *Pharmacol. Rev.* **2001**, *53*, 283–318.
[22] M. Vaccaro, A. Accardo, D. Tesauro, G. Mangiapia, D. Löf, K. Schillén, O. Söderman, G. Morelli, L. Paduano, *Langmuir* **2006**, *22*, 6635–6643.
[23] L. A. Feigin, D. I. Svergun, *Structure analysis by small-angle X-ray and neutron scattering*, Plenum, New York, **1987**.
[24] G. Mangiapia, A. Accardo, F. Lo Celso, D. Tesauro, G. Morelli, A. Radulescu, L. Paduano, *J. Phys. Chem. B* **2004**, *108*, 17 611–17 617.
[25] A. Vergara, L. Paduano, V. Vitagliano, R. Sartorio, *Phys. Chem. Chem. Phys.* **1999**, *1*, 5377–5383.
[26] L. Aloj, E. Jagoda, L. Lang, C. Caraco, R. D. Neumann, C. Sung, W. C. Eckelman, *J. Nucl. Med.* **1999**, *40*, 1547–1555.
[27] A. Fritze, F. Hens, A. Kimpfler, R. Schubert, R. Peschka-Süss, *Biochim. Biophys. Acta Biomembr.* **2006**, *1758*, 1633–1640.
[28] A. Accardo, D. Tesauro, G. Mangiapia, C. Pedone, G. Morelli, *Biopolymers* **2007**, *88*, 115–121.
[29] L. Aloj, C. Caraco, M. Panico, A. Zannetti, S. Del Vecchio, D. Tesauro, S. De Luca, C. Arra, C. Pedone, G. Morelli, M. Salvatore, *J. Nucl. Med.* **2004**, *45*, 485–494.
[30] L. Schmitt, C. Dietrich, *J. Am. Chem. Soc.* **1994**, *116*, 8485–8491.
[31] W. C. Chang, P. D. White, *Fmoc solid phase peptide synthesis*, Oxford University Press, Oxford, **2000**.
[32] A. M. Kotlarchyk, S. H. Chen, *J. Chem. Phys.* **1983**, *79*, 2461–2469.
[33] B. D. Schwahn, D. Richter, M. Lin, L. J. Fetters, J. Lewis, *Macromolecules* **2002**, *35*, 3762–3768.
[34] C. G. Ma, D. J. Barlow, M. J. Lawrence, R. K. Heenan, P. Timmins, *J. Phys. Chem. B* **2000**, *104*, 9081–9085.
[35] J. Jansson, K. Schillén, G. Olofsson, R. Cardoso da Silva, W. J. J. Loh, *J. Phys. Chem. B* **2004**, *108*, 82–92.
[36] B. J. Berne, R. Pecora, *Dynamic Light Scattering: with Application to Chemistry, Biology and Physics*, Dover Mineola, New York, **2000**.
[37] R. J. Young, P. A. Lovell, *Introduction to Polymers*, Chapman & Hall, London, **1996**.
[38] P. Stepánek, *Dynamic Light Scattering* (Ed.: W. Brown), Oxford University Press, Oxford, **1993**.
[39] R. Johnsen, W. Brown, Bloomfield, *Laser Light Scattering in Biochemistry* (Eds.: S. E. Harding, D. B. Sattelle), Royal Society of Chemistry, Cambridge, **1992**, p. 77.
[40] O. Glatter, G. Scherf, K. Schillén, W. Brown, *Macromolecules* **1994**, *27*, 6046–6054.
[41] M. Almgren, K. Edwards, J. J. Gustafsson, *Curr. Opin. Colloid Interface Sci.* **1996**, *1*, 270–278.
[42] P. Skehan, R. Storeng, D. Scudiero, A. Monks, J. McMahon, D. Vistica, J. T. Warren, H. Bokesch, S. Kenney, M. R. Boyd, *J. Natl. Med. Assoc. J. Natl. Cancer Inst.* **1990**, *82*, 1107–1112.

Received: September 26, 2007
Revised: November 20, 2007
Published online on January 2, 2008

